Table S1: Lithophile Isotope Data in Raivavae and Rapa Basalts

Location	**Sample name**	**$^{87}Sr/^{86}Sr$**	**$^{143}Nd/^{144}Nd$**	**$^{206}Pb/^{204}Pb$**
Raivavae	RVV 360a			20.82
Rapa	RPA 367	0.70410	0.512740	18.95
	RPA 473		0.512772	
	RPA 488	0.70394	0.512775	19.11
	RPA 502			19.28

Sr, Nd, and Pb analyses were performed at University of Texas, Austin using analytical procedures previously reported in Lassiter et al., 2003.

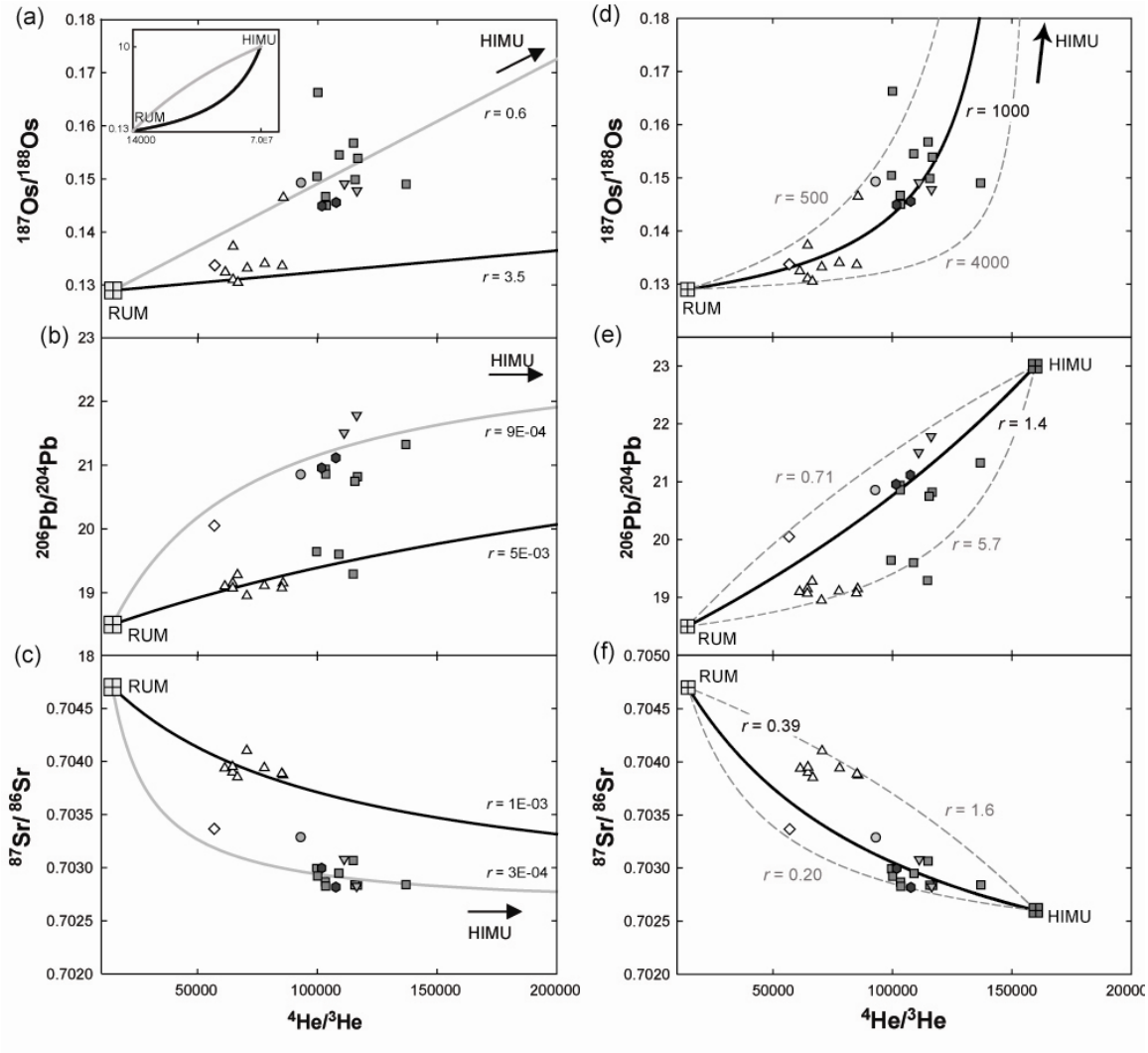

Figure S1 Cook-Austral data are shown in He-Os (a,d), He-Pb (b,e) and He-Sr (c,f) isotopic space, along with models of two-component mixing between RUM and the two HIMU components considered in the discussion. Symbols as in Figure 4. Isotopic compositions and abundances of the components are given in section 4.3.1 and Figure 8 caption. Panels (a-c) show mixing between RUM and the HIMU component with $^{4}He/^{3}He = 7 \times 10^{7}$, while panels (d-f) show mixing with the HIMU component at $^{4}He/^{3}He = 160\ 000$. We first determine $r_{He\text{-}Os}$ values, defined as $(^{188}Os/^{3}He)_{RUM}/(^{188}Os/^{3}He)_{HIMU}$, that are most consistent with the HIMU and EM lavas (panels a,d). Using X/Os ratios in

the two components (where X is Sr, Nd, or Pb), $r_{He\text{-}Os}$ is propagated through to mixing in He-X isotopic space to generate an internally consistent set of mixing lines with respect to He concentrations. For instance, $r_{He\text{-}Sr} = r_{He\text{-}Os} * (^{86}Sr/^{188}Os)_{RUM}/(^{86}Sr/^{188}Os)_{HIMU}$. The *r* values are indicated in the figure. The two-component mixing calculations indicate that the major trends in the data can be explained by mixing between RUM and a HIMU mantle component, with the EM-type lavas having a higher proportion of RUM in the mixture. However, a third component is most likely involved (see Discussion 4.3). Note that the mixing curvatures consistently suggest that Rapa lavas have higher $[(X/^{3}He)_{RUM}]/[(X/^{3}He)_{HIMU}]$. Since magmatic degassing will affect the ^{3}He concentrations, but not the abundances of non-volatile elements, the lower ratios may reflect a higher degree of degassing prior to mixing (see Discussion).

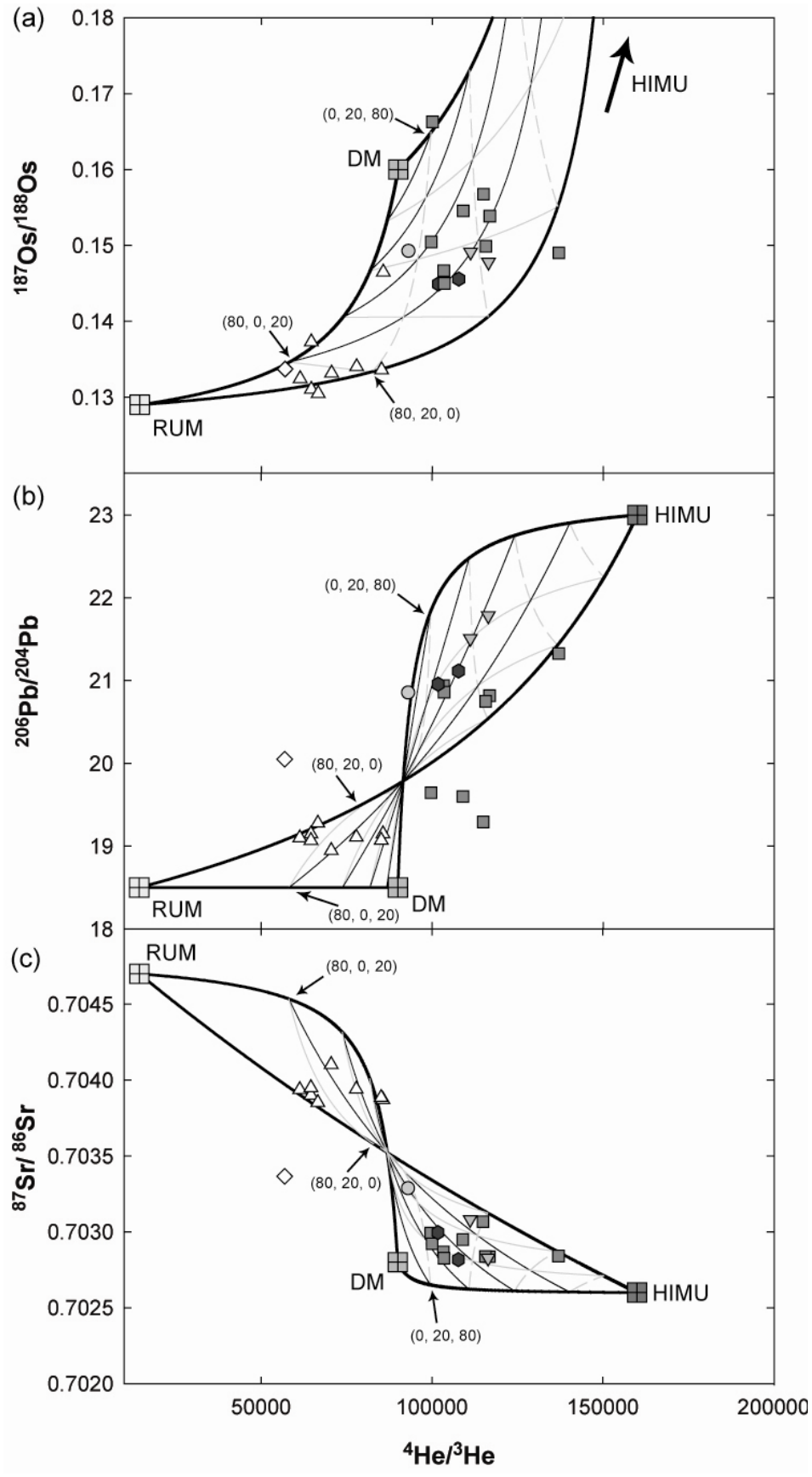
(a)
(b)
(c)
$^{187}Os/^{188}Os$
$^{206}Pb/^{204}Pb$
$^{87}Sr/^{86}Sr$
$^{4}He/^{3}He$
RUM
DM
HIMU
(0, 20, 80)
(80, 0, 20)
(80, 20, 0)
0.18
0.17
0.16
0.15
0.14
0.13
23
22
21
20
19
18
0.7045
0.7040
0.7035
0.7030
0.7025
0.7020
50000
100000
150000
200000

Figure S2: Three-component mixing with the HIMU component $^{4}He/^{3}He$ = 160 000 is illustrated in He and (a) Os, (b) Pb, and (c) Sr isotopic space. Symbols as in Figure 4; end-member isotopic compositions are shown in the figures and listed in section 4.3.1. Elemental abundances are found in the caption for Figure 8, along with an explanation of our three-component mixing calculations. $[(^{188}Os/^{3}He)_{RUM} : (^{188}Os/^{3}He)_{HIMU} : (^{188}Os/^{3}He)_{DM}]$ = [1 : 5.1E-04 : 0.16] for HIMU component $^{4}He/^{3}He$ = 160 000. The surface contours represent a constant proportion of component X in the mixture (solid black line X = DM; dashed grey line X = HIMU; solid grey line X = RUM). Intersections between some contours have been labeled with ordered triples (%RUM, %HIMU, %DM) to give a sense of relative proportions. Our calculations demonstrate that regardless of the helium isotopic composition of the HIMU component, the Cook-Austral data are consistent with three-component mixing between RUM, HIMU and DM components. Furthermore, a component with characteristics more primitive than either DM or HIMU is clearly required.